

See discussions, stats, and author profiles for this publication at: <https://www.researchgate.net/publication/272101064>

# A novel class of ruthenium-based photosensitizers effectively kills in vitro cancer cells and in vivo tumors

Article in *Photochemical and Photobiological Sciences* · February 2015

DOI: 10.1039/C4PP00438H

CITATIONS

19

READS

114

7 authors, including:



**Yaxal Arenas**

University Health Network

9 PUBLICATIONS 68 CITATIONS

[SEE PROFILE](#)



**Pavel Kaspler**

Theralase Technologies Inc.

20 PUBLICATIONS 194 CITATIONS

[SEE PROFILE](#)



**Lothar Lilge**

Princess Margaret Cancer Centre AND Univer...

289 PUBLICATIONS 4,211 CITATIONS

[SEE PROFILE](#)

Some of the authors of this publication are also working on these related projects:



Optical Breast Cancer Risk Assessment and Pre-screening [View project](#)



Low Level Laser mediated Biomodulation Therapy [View project](#)



Cite this: DOI: 10.1039/c4pp00438h

## A novel class of ruthenium-based photosensitizers effectively kills *in vitro* cancer cells and *in vivo* tumors†

Jamie Fong,<sup>a</sup> Kamola Kasimova,<sup>b</sup> Yaxal Arenas,<sup>a</sup> Pavel Kaspler,<sup>a</sup> Savo Lazic,<sup>a</sup> Arkady Mandel<sup>a</sup> and Lothar Lilge<sup>\*b,c</sup>

The photo-physical and photo-biological properties of two small (<2 kDa), novel Ru(II) photosensitizers (PSs) referred to as TLD1411 and TLD1433 are presented. Both PSs are highly water-soluble, provide only very limited luminescence emission at 580–680 nm following excitation at 530 nm, and demonstrate high photostability with less than 50% photobleaching at radiant exposures  $H = 275 \text{ J cm}^{-2}$  (530 nm irradiation). It was previously shown that these two photosensitizers exhibit a large singlet oxygen ( $^1\text{O}_2$ ) quantum yield ( $\Phi(\Delta) \sim 0.99$  in acetonitrile). Their photon-mediated efficacy to cause cell death ( $\lambda = 530 \text{ nm}$ ,  $H = 45 \text{ J cm}^{-2}$ ) was tested *in vitro* in colon and glioma cancer cell lines (CT26.WT, CT26.CL25, F98, and U87) and demonstrated a strong photodynamic effect with complete cell death at concentrations as low as 4 and 1  $\mu\text{M}$  for TLD1411 and TLD1433, respectively. Notably, dark toxicity was negligible at concentrations less than 25 and 10  $\mu\text{M}$  for TLD1411 and TLD1433, respectively. The ability of the PSs to initiate Type I photoreactions was tested by exposing PS-treated U87 cells to light under hypoxic conditions ( $p\text{O}_2 < 0.5\%$ ), which resulted in a complete loss of the PDT effect. *In vivo*, the maximum tolerated doses 50 (MTD50) were determined to be 36  $\text{mg kg}^{-1}$  (TLD1411) and 103  $\text{mg kg}^{-1}$  (TLD1433) using the BALB/c murine model. *In vivo* growth delay studies in the subcutaneous colon adenocarcinoma CT26.WT murine model were conducted at a photosensitizer dose equal to 0.5 and 0.2 MTD50 for TLD1411 and TLD1433, respectively. 4 hours post PS injection, tumours were irradiated with continuous wave or pulsed light sources ( $\lambda = 525\text{--}530 \text{ nm}$ ,  $H = 192 \text{ J cm}^{-2}$ ). Overall, treatment with continuous wave light demonstrated a higher tumour destruction efficacy when compared to pulsed light. TLD1433 mediated PDT resulted in statistically significant longer animal survival compared to TLD1411. Two-thirds of TLD1433-treated mice survived more than 100 days ( $p < 0.01$ ) whereas TLD1411-treated mice did not survive longer than 20 days. Here we present evidence that two novel PSs have very potent photo-biological properties and are able to cause PDT-mediated cell death in both *in vitro* cell culture models and *in vivo* tumour regression.

Received 24th November 2014,

Accepted 27th January 2015

DOI: 10.1039/c4pp00438h

www.rsc.org/ppp

## Introduction

Photodynamic therapy (PDT) has been advanced as a potential therapy for a variety of cancers, either as a sole treatment or in conjunction with surgery, chemotherapy, and/or radiation.<sup>1</sup> PDT is a minimally invasive technique with its efficacy determined by at least three dose parameters: a photosensitizer

(PS), light energy- and intensity-density, and oxygen. Ideally, systemic or local administration of a PS will lead to an accumulation into the target tissue.<sup>2,3</sup> Tissue irradiation with light of a wavelength specific to the PS's absorption profile generates reactive species *via* Type I (oxygen independent) or Type II (oxygen dependent) photochemical reactions, subsequently leading to cell death *via* apoptosis or necrosis.<sup>4</sup> Owing to the short diffusion distances for reactive oxygen species (ROS) and other radicals generated, the PS concentration and its subcellular localization are an important aspect towards establishing effective tumour control.<sup>5,6</sup>

To attain the best efficacy of PDT for the widest range of tumours, PSs with a range of photo-physical and photo-biological attributes may need to be developed, whereby these attributes include specific cellular and subcellular targeting,

<sup>a</sup>Theralase Technologies, 1945 Queen St. East, Toronto, ON M4L 1H7, Canada

<sup>b</sup>Princess Margaret Cancer Centre/University Health Network, 101 College Street 15-310, Toronto, ON M5G 1L7, Canada. E-mail: llilge@uhnresearch.ca

<sup>c</sup>University of Toronto, Department of Medical Biophysics, 610 University Ave., Toronto, ON M5G 2M9, Canada

†Electronic supplementary information (ESI) available. See DOI: 10.1039/c4pp00438h

maintenance of high cytotoxic load in oxygen-depleted environments, and activation by light with sufficient penetration depth in the target tissue. PSs localized in lysosomes, mitochondria, or nuclei have shown promising results in eliciting apoptosis and/or necrosis.<sup>7</sup> For nuclear targets, the binding of a PS to DNA can potentially disrupt replication and transcription, leading to structural modifications of the chromatin and ultimately apoptosis.<sup>8</sup>

While generally continuous wave (cw) lasers are utilized for PDT, 2 photon PDT<sup>9,10</sup> is considered to achieve higher tissue penetration, although the maximum power density allowable for cw light is limited by heat dissipation constraints at the tissue surface, often the skin.<sup>11</sup> By virtue of the dark periods between pulses, higher power density can be used in pulsed light PDT while still maintaining a lower average power, minimizing local tissue heating.<sup>12</sup>

High absorption cross-sections and their relatively long triplet state lifetimes might capitalize on the use of pulsed light sources for PDT applications. The modular nature of the Ru(II) coordination sphere enables the incorporation of engineered ligands resulting in both highly oxidizing and/or reducing excited states as required for Type I photoprocesses.<sup>13</sup>

While porphyrins, reduced porphyrins (including chlorins and bacteriochlorins) and phthalocyanines, with or without a central metal ion, form the basis of traditional PS for PDT,<sup>6</sup> coordination complexes derived from Ru(II) have garnered considerable attention as photosensitizers for solar cells, the direct oxidation of water,<sup>14,15</sup> and also medical applications. In particular, the DNA intercalating abilities<sup>16</sup> of Ru(II) complexes have been shown to induce single and double stranded breakage *in vitro* following blue light activation as evidenced by an increase in the number of DNA fragments following *in vitro* PDT effects.<sup>17–19</sup> Cisplatin-like covalent binding to DNA following light activation for triplet metal-to-ligand charge transfer (<sup>3</sup>MLCT) in *cis*-[Ru(phenylpyridine)(1,10-phenanthroline)(CH<sub>3</sub>CN)(2)](+) or Ru(II) polypyridyl biquinoline ligand complexes was demonstrated for particular irradiation conditions.<sup>17,20</sup> Photoactivation based on energy or electron transfer is achieved *via* <sup>3</sup>MLCT excited state such as [Ru(bpy)<sub>3</sub>]<sup>2+</sup> or its derivatives. They can generate excited state lifetimes of about 1 μs in deoxygenated solution. Longer lifetimes have also been reported for low-lying triplet intraligand <sup>3</sup>IL excited states.

One of the critical issues towards translation for clinical applications is the need to achieve absorption beyond the commonly reported 420 nm. For Ru(II) 2,3-bis(2-pyridyl)-benzoquinoline pyridine complexes, the delocalized nature of the 2,3-bis(2-pyridyl)-benzoquinoline is thought to provide absorption into the red range of the optical spectrum.<sup>21</sup> A different approach to obtain long wavelength absorption can be provided through the use of <sup>3</sup>IL excited states to achieve longer excited state lifetimes in Ru(II) polypyridyl complexes and absorption into the red part of the optical spectrum, albeit their use *in vitro* or *in vivo* has not been reported as often white light excitation is utilized.<sup>22</sup>

The ability to prepare and isolate these Ru(II) PSs as single entities, along with their absorption of visible light and high <sup>1</sup>O<sub>2</sub> quantum yields,<sup>23</sup> is in part responsible for this interest. Their low *in vivo* toxicity and modular design are salient features for clinical applications. PS conjugation to ruthenium could also improve cellular uptake and possesses DNA binding and photocleavage activities.<sup>24</sup> With regard to the latter, pseudo-octahedral Ru(II) complexes had been designed with three bidentatediimine ligands. In these complexes, two identical ligands offer stability for the third ligand showing an affinity for DNA. Thus they exhibit potent photoreactivity, which translates to excellent *in vitro* PDT, capable of providing a high <sup>1</sup>O<sub>2</sub> quantum yield upon light irradiation.<sup>25</sup>

The paucity of available literature regarding whether pulsed sources are more effective than cw systems<sup>26</sup> and on the clear advantages that might be gained with specially designed Ru(II)-based PSs has led to an active area of research. Herein, we report a new class of Ru(II)-based PSs for PDT, using two complexes of the type [Ru(LL)<sub>2</sub>(LL')]<sub>2</sub><sup>+</sup>, where LL is 2,2'-bipyridine (bpy) in the case of TLD1411 or 4,4'-dimethyl-2,2'-bipyridine (dmb) in TLD1433 and LL' is 2-(2',2'':5'',2'''-terthiophene)-imidazo[4,5-*f*][1,10] phenanthroline<sup>22,27,28</sup> (IP-TT). We determined the photo-physical properties of TLD1411 and TLD1433 and highlight their efficacy in causing *in vitro* cancer cell death. The photosensitizing effect under normoxic and hypoxic (<0.5% pO<sub>2</sub>) conditions was studied, and we examined whether pulsed, monochromatic excitation can be used to populate higher excited states for the exploitation of non-thermal excited state photoprocesses. Importantly, we demonstrate the utility of this class of PSs as PDT agents against colon carcinoma in an *in vivo* mouse model showing that for TLD1433 a high fraction of long-term survivors was attainable.

## Materials and methods

### Photosensitizers

TLD1411 and TLD1433 are Ru(II)-based photodynamic compounds with a general structure of [Ru(LL)<sub>2</sub>(LL')]<sub>2</sub><sup>+</sup>, where LL is 2,2'-bipyridine (bpy) for TLD1411 or 4,4'-dimethyl-2,2'-bipyridine (dmb) for TLD1433 and LL' is 2-(2',2'':5'',2'''-terthiophene)-imidazo[4,5-*f*][1,10]phenanthroline (IP-TT) for both. The class to which these PSs belong is characterized by the incorporation of a key oligothiophene unit at the C2 position of imidazo[4,5-*f*][1,10] phenanthroline (IP). The number of thiophenes in this unit is defined as *n* and increases from one until yield becomes a limiting factor. A previous report<sup>29</sup> provides complete structural and chemical details. Synthesis steps have been described previously<sup>29,30</sup> and include the preparation of IP-TT from commercially available starting materials and subsequent complexation to Ru(bpy)<sub>2</sub>Cl<sub>2</sub> or Ru(dmb)<sub>2</sub>Cl<sub>2</sub>, prepared according to established methods.<sup>31</sup> Previous studies have demonstrated that these PSs have a nuclear localization in cells *in vitro* and a high affinity for DNA isolates of up to 10<sup>8</sup> M<sup>-1</sup>.<sup>23</sup> They exhibit strong excited state reduction and oxidation potentials. For example, the reduction and oxidation

potentials for TLD1411 and TLD1433 are of the order of 1.31 and  $-0.87$  V, respectively,<sup>28</sup> allowing for guanine oxidation and cytosine/thymine reduction upon photoactivation. DNA photocleavage has also been demonstrated *in vitro* and is enhanced by endogenous reductants such as glutathione, resulting in double stranded DNA breaks.<sup>30</sup>

### PS absorbance and luminescence emission measurements

The absorption spectra in ddH<sub>2</sub>O were recorded from 300 nm to 800 nm ( $5 \mu\text{M}$  and  $6.7 \mu\text{M}$  for TLD1411 and TLD1433, respectively) using a dual beam spectrophotometer (Cary 300 Bio UV-Visible spectrophotometer, Varian Inc., FL 07033947, CA, USA). To measure the photostability, the PSs were dissolved in either ddH<sub>2</sub>O or a solution with 5 times the PS concentration of bovine serum albumin (BSA) (Sigma, Oakville, Canada) ( $25 \mu\text{M}$  for TLD1411,  $34 \mu\text{M}$  BSA for TLD1433). PSs were irradiated with the green LED light source at  $78 \text{ mW cm}^{-2}$  for 60 minutes. The OD at the longest wavelength maxima ( $525 \pm 25 \text{ nm}$  for TLD1411,  $423 \pm 25 \text{ nm}$  for TLD1433) was measured every 5 minutes and plotted against the absorbed photon density.

These Ru(II) complexes are known to have long lived excitation states and emit phosphorescence in deoxygenated environments.<sup>27</sup> Therefore, we have not determined the lifetime or the state from which the emission occurs under our different conditions and hence we refer only to luminescence emission. For luminescence measurements a dual grating spectrofluorometer (Fluorolog, Horiba Jobin Yvon, NJ, USA) was used on solutions adjusted to a maximum OD of 0.2 at the excitation wavelength. TLD1411 was excited at 461 nm, and the emission was measured from 487 nm to 800 nm, whereas TLD1433 was excited at 480 nm and the emission was measured from 520 nm to 800 nm. Due to the low quantum yield and the wide absorption band, an excitation bandwidth of 4 nm and 5 nm was used for both PSs. To permit the use of higher concentrations of the PS a 3 mm path length cuvette was used. The PS luminescence based detection limit was determined for each PS by establishing a calibration curve in the appropriate solvent according to Lilge *et al.*<sup>32</sup> Briefly, the luminescence for both PSs, starting at the MTD50 dose and following 10 dilution steps, was determined and plotted. For each sample, 4 scans (with a signal integration time of 0.5 second) were averaged to create the luminescence system calibration according to an established procedure.

### Cell lines and reagents

Cell lines were purchased from ATCC (Manassas, VA): mouse colon fibroblast, CT26 wild type (CT26.WT, #CRL-2638), CT26.CL25 (#CRL-2639); human brain, U87MG (U87, #HTB-14); and rat glioblastoma, F98 (#CRL-2397). The short tandem repeat (STR) profiles for all cell lines have been verified.

Cells were cultured in RPMI 1640 medium (CT26.WT, CT26.CL25) or DMEM medium (U87, F98) supplemented with 10% fetal bovine serum and 1% penicillin ( $5000 \text{ units ml}^{-1}$ ) and streptomycin ( $5000 \mu\text{l ml}^{-1}$ ) (all from Gibco, Invitrogen, CA, USA) in  $75 \text{ cm}^2$  flasks (Falcon, Invitrogen, CA, USA) and main-

tained at  $37 \text{ }^\circ\text{C}$  in 5% CO<sub>2</sub>. All media used for culturing and plating cells contained phenol red, except DMEM medium used for PDT. Cells were passaged at 80% confluence, and complete medium exchange was performed every 2–3 days. Cells were used from passage number 6 to 27.

### *In vitro* PDT

15 000 cells were plated per well in duplicate 96-well plates (Falcon, Invitrogen, CA, USA) 24 hours prior to experiments using  $200 \mu\text{L}$  of cell suspension per well. The following day, the medium was replaced with medium plus TLD1411 or TLD1433 at varying concentrations. Following 4–6 hours of PS loading, a time interval shown not to alter the cell kill, the unbound PS was removed by complete medium exchange with fresh sodium pyruvate-free medium, followed by PDT light irradiation. Irradiation of the entire 96-well plate was conducted using a green LED emitting at  $525 \pm 25 \text{ nm}$  (FWHM) (model LZ4-00G100, LED Engin, San Jose, CA, USA) provided by Theralase Inc. (Toronto, ON, Canada). An energy density of  $45 \text{ J cm}^{-2}$  was delivered at the fluency rate of  $108 \text{ mW cm}^{-2}$ . Irradiance was homogeneous to within 12% across all wells. Active air-cooling maintained the temperature of the tissue culture medium within  $3 \text{ }^\circ\text{C}$  above ambient temperature. After irradiation, cells were maintained in an incubator at  $37 \text{ }^\circ\text{C}$  under an atmosphere of 5% CO<sub>2</sub> for 20 hours in the dark. Cell viability was measured in duplicate 96-wells, using the Presto Blue Cell Viability assay<sup>33</sup> (Invitrogen, CA, USA), according to the manufacturer's protocol, with the readout provided by a SpectroMax M5 (Molecular Devices, Sunnyvale, CA, USA).

For hypoxic experiments, all solutions used were kept under hypoxic conditions for at least 24 hours prior to the experiment. To facilitate attachment, the cells containing 96 well plates were transferred to a hypoxic chamber (InvivoO<sub>2</sub> 400 Ruskin Technology Ltd, UK) 4 hours post normoxic seeding. The plates remained under hypoxic conditions for 24 hours prior to PDT light irradiation. The hypoxic chamber had an atmosphere of 0.5% O<sub>2</sub>, 5% CO<sub>2</sub>, balanced with N<sub>2</sub>, at  $37 \text{ }^\circ\text{C}$  and 95% humidity. Similar to normoxic conditions, medium with PS was added and replaced with fresh medium following the 4–6 hour PS loading. Cells were kept for 2 hours at 0.1% O<sub>2</sub> to further reduce the available oxygen in the experimental well. The oxygen diffusion times across the  $\sim 3 \text{ mm}$  liquid column are much shorter than the exposure times of  $\sim 7 \text{ min}$  and hence re-oxygenation from the outside environment had to be limited without compromising PDT independent cell survival. Following irradiation, cells were kept at 0.5% O<sub>2</sub> for 24 hours until cell viability measurements were performed. For all procedures conducted under normal, ambient conditions (light irradiation, cell death measurements), the plates containing hypoxic cells were sealed airtight with an oxygen-impermeable adhesive film (Evergreen Scientific, USA). When the plates were returned to hypoxic conditions, sealing was removed and the plate covers were replaced. This did not alter the  $p\text{O}_2$  in the experimental wells, as tested by a colorimetric assay.<sup>34</sup>

### *In vitro* scavengers

To assess the contribution of hydroxyl radicals and  $^1\text{O}_2$ , the cells were loaded with PS in the presence of either *N,N'*-dimethylthiourea (DMTU), a scavenger of hydroxyl radicals (10–40  $\mu\text{M}$ ) or sodium azide, a scavenger of singlet oxygen (2  $\mu\text{M}$ ). Before PDT, but after removal of PS, freshly prepared solutions of the scavengers were added to the cells and then replaced with fresh medium following PDT activation.

### *In vivo* murine model

8–10 week old BALB/C mice were used for *in vivo* experiments. All animal experiments were carried out in accordance with protocols approved by the Animal Care Committee at the University Health Network, ON, Canada (IACUC approval date 08/03/2012, assurance number A5408-01). All animals were housed in the vivarium with water and food supplied *ad libitum* in a 12 hour day/night cycle. For CT26.WT murine colon carcinoma cell injections, mice were anaesthetized with Isoflurane (5% induction, 1.5% maintenance) and one hind leg was shaved. Mice were subcutaneously injected with 300 000 to 350 000 cells per mouse in 100  $\mu\text{L}$  PBS into the dorsal area of the leg over 30 seconds. The tumour size was measured in two dimensions with a manual Vernier calliper every 2–3 days. When tumour size reached 5–6 mm TLD1411 or TLD1433 was intratumour (IT) injected by an estimate of 100  $\mu\text{L}$  at a body weight of 20 g using a syringe pump (New Era Pump Systems Inc., #NE1000) at 0.01  $\text{ml min}^{-1}$ . Control mice were IT injected with sterile saline. After 4 hours the tumours were irradiated as described below, while mice were under anaesthesia with Isoflurane (1.5% in  $\text{O}_2$ ).

### Determination of MTD50 values

The MTD50 for both PSs was determined in non-tumour bearing animals by administering a series of increasing and decreasing drug doses, starting in three mice at a concentration hundred times below the presumed MTD50 according to *in vitro* studies, following the Guidelines for the Testing of Chemicals 2009 (OECD/OCDE-2009). Both male and female BALB/c mice, aged 8–10 weeks old, received an intraperitoneal (IP) injection of TLD1411 or TLD1433 dissolved in a 250  $\mu\text{L}$  volume of  $\text{dH}_2\text{O}$  per 20 g mouse weight. Animals were observed constantly for 2 hours, then frequently for 6 hours and periodically for up to two weeks. Clinical scoring parameters including changes in respiration, complexion, heart rate, and any neurological symptoms were recorded. An overall classification of clinical symptoms as none, mild, moderate, or severe, based on the Federation for Laboratory Animal Science Associations (FELASA) endpoint guidelines, was determined for each animal tested.<sup>35,36</sup> If, within the first 48 hour interval post drug injection, two or more mice appeared healthy, the subsequent batch of three mice were administered a 5 times higher PS dose. If two or more mice showed signs of distress, the subsequent batch of three mice received half the previous dose. This reduced dose batch was monitored for the entire two week observation period. This cycle repeated itself for all

additional batches of mice with the exception that further dose progressions were increased by a factor of 2.5 instead of 5 if two or more mice appeared healthy. The MTD50 was identified as the dose that produced moderate severity in the final animal group tested.

### PS biodistribution

8–10 week old BALB/c mice were injected with CT26.WT tumour cells in the hind leg as described above. When tumours reached approximately 5–6 mm in diameter, mice were anaesthetized with Isoflurane (5% induction, 1.5% maintenance) and were administered TLD1411 or TLD1433 at 1/2 MTD50 doses or vehicle alone ( $\text{ddH}_2\text{O}$ ), in a volume of 250  $\mu\text{L}$  per 20 g mouse for IP injections and 100  $\mu\text{L}$  per 20 g mouse for IT injections using a 27 G needle and a syringe pump (New Era Pump Systems Inc., Model NE1000) set at an injection rate of 10  $\mu\text{L}$  per minute. 4 or 24 hours post PS injection, mice were euthanized by cervical dislocation following anaesthesia with 5% Isoflurane. Various tissue samples comprising brain, heart, kidney, liver, muscle, skin near tumour, muscle near tumour, and tumour were collected. Each sample was rinsed in saline to remove blood. Excess liquid was removed by paper blotting before tissues were snap frozen in liquid nitrogen. All samples were stored at  $-80^\circ\text{C}$  until analysis.

Tissue samples were solubilised as described previously.<sup>32</sup> Tissues were chopped into  $\sim 0.05$  g pieces and weighed. 1 ml (for  $<0.01$  g tissue) or 2 ml (for 0.1–0.4 g tissue) solvable (Perkin Elmer, Woodbridge, Canada) was added to the samples and incubated on top of a shaking platform that was placed in a water bath set at  $-50^\circ\text{C}$  (Gyrotory Water Bath Shaker, New Brunswick Scientific, USA) for 1 hour. Tissues were then homogenized using a tissue homogenizer (Tissue Tearor, Biospec Products Inc., Canada) by performing 3 up and down pulses. An additional 0.5 ml of solvable and 1.5 ml of distilled  $\text{H}_2\text{O}$  (for  $<0.1$  g tissue) or 1 ml solvable and 3 ml distilled  $\text{H}_2\text{O}$  (for 0.1–0.4 g tissue) was added to the homogenate and further incubated in the warm water bath for 1 hour. Samples were transferred to plastic cuvettes (VWR, Mississauga, ON) and luminescence emission was measured using the above described parameter settings. The tissue concentration was calculated according to eqn (1) in Lilge *et al.*<sup>32</sup>

### *In vivo* PDT

PDT was performed 4 hours following IT injections as described above. Each mouse was anaesthetized with Isoflurane (5% induction, 1.5% maintenance) and rested on a platform placed above the light source. The mouse was positioned so that the tumour was above a 1.3 cm diameter aperture in the platform allowing light exposure. A cooled water blanket, set to  $\sim 30^\circ\text{C}$ , was lightly placed on top of the mouse to assist in the heat removal from energy absorbed by the vasculature.

For PDT light activation, cw and pulsed, or here quasi-cw, light sources were used. A single light power LED (model LZ4-00G100, LED Engin, San Jose, CA, USA) emitting at 525 nm, providing an irradiance of 200  $\text{mW cm}^{-2}$  at 0.5 Hz and 50% duty cycle, achieved by a chopper (Stanford Research Systems,

Inc., model SR540 Chopper Controller, CA, USA), required 32 minutes to deliver a total radiant exposure of  $192 \text{ J cm}^{-2}$  to the skin above the tumour. For pulse PDT activation, the 532 nm emitting, quasi-cw light Verdi laser (Coherent, V-55 Diode Pumped Lasers, CA, USA), featuring picosecond pulses at 40 MHz repetition rate, was employed. The duty cycle of this laser is  $\sim 0.01$ , resulting in a peak power of  $18 \text{ W cm}^{-2}$  and an average power of  $<200 \text{ mW cm}^{-2}$ . A delivery of the same radiant exposure of  $192 \text{ J cm}^{-2}$  at 0.5 Hz and 50% duty cycle required 40 minutes.

Tumour long ( $a$ ) and short axes ( $b$ ), respectively, were measured daily following PDT and the tumour volumes were calculated according to  $V = 4\pi/3 \times [(a + b)/4]^3$ . Any physical changes in the mice and/or tumours were noted. Mice were euthanized if the tumour's long axis reached 12 mm. Kaplan–Meier plots noted days post PDT until the determined end point.

### Statistical analysis

In the cell viability measurements following *in vitro* PDT experiments, the recorded fluorescence was converted to a percentage of viable cells relative to the number of viable control cells (no PS, no light under normoxic or hypoxic conditions). Cell death was calculated as total cell death minus dark toxicity and light only toxicity. Dark toxicity was considered as cell death elicited by the PS without light or PS plus the scavenger mixture without light. The significance of PDT treatment or dark toxicity was determined by analysing 95% confidence intervals of  $\text{LD}_{50}$  doses calculated from a non-linear fit in Prism 5.00. Non-overlapping confidence intervals denoted a significant difference,  $p < 0.05$ .

Kaplan–Meier curves were established for the survival analyses. An average of 5 mice was used for each condition. One-way ANOVA and Mantel–Cox (Kaplan–Meier) tests were conducted to test for significance. Tests were considered significant with  $p$  values of  $<0.05$ .

## Results

The absorption spectra of TLD1411 ( $5 \mu\text{M}$ ) and TLD1433 ( $6.7 \mu\text{M}$ ) in  $\text{ddH}_2\text{O}$  are very similar (see Fig. SI 1†) with the main absorbance ranges from 300–600 nm for TLD1411 and 300–550 nm for TLD1433, and long-wavelength absorption peak maxima at 416 nm for both PSs. TLD1411 has a slightly higher molar extinction coefficient between 525 and 532 nm compared to TLD1433. Neither PS absorbs red light.

The luminescence emission spectra from the two PSs display a broad peak centred at  $\sim 625 \text{ nm}$  (Fig. SI 2†) with no discernible fine structure. The  $^1\text{O}_2$  quantum yields are approximately unity;<sup>29,30</sup> hence, the weak luminescence emissions are not surprising. The emission of both PSs was linear across the anticipated concentrations used in tissue extraction experiments (Fig. SI 3†).

PS photobleaching was assessed for samples with an OD 0.2 to avoid inter-filter effects. The samples were irradiated

with 525 nm light at  $78 \text{ mW cm}^{-2}$  for 60 minutes to exceed the maximum radiance exposure delivered in subsequent experiments while the absorbance was measured every 5 minutes. TLD1411 photobleached by approximately 65% and TLD1433 photobleached by 50% after absorption of more than  $3 \times 10^{21} \text{ h}\nu \text{ cm}^{-3}$  in water (data not shown). Both PSs showed improved photostability, with a reduction of 40% in absorption when irradiated in the presence of 5 times molar excess of BSA (Fig. SI 4†), an environment that mimics biological conditions more accurately than aqueous solutions of PS alone. TLD1411 and TLD1433 pre-irradiated with  $200 \text{ J cm}^{-2}$  in the presence of BSA prior to tissue culture addition for incubation did not modify the efficacy of PDT (data not shown).

The potential of TLD1411 and TLD1433 as PSs for PDT was assessed *in vitro* in four cancer cell lines: CT26.WT (murine colon carcinoma), CT26-CL25 (immunogenic murine colon carcinoma), F98 (rat glioma), and U87 (human glioblastoma). Cells were incubated with 0–180  $\mu\text{M}$  TLD1411 or TLD1433 for 4–6 hours (Fig. 1). Dark toxicity was minimal for the concentration range employed in these studies, *i.e.*, less than 10% for up to 10  $\mu\text{M}$  concentration. A concentration dependent, strong photodynamic effect was observed for all cell lines tested, reaching 100% cell kill with the exception of F98 treated with TLD1411 (Fig. 1). The minimal concentration sufficient for 100% cell kill of U87 or CT26.WT was 4  $\mu\text{M}$  for TLD1411 and

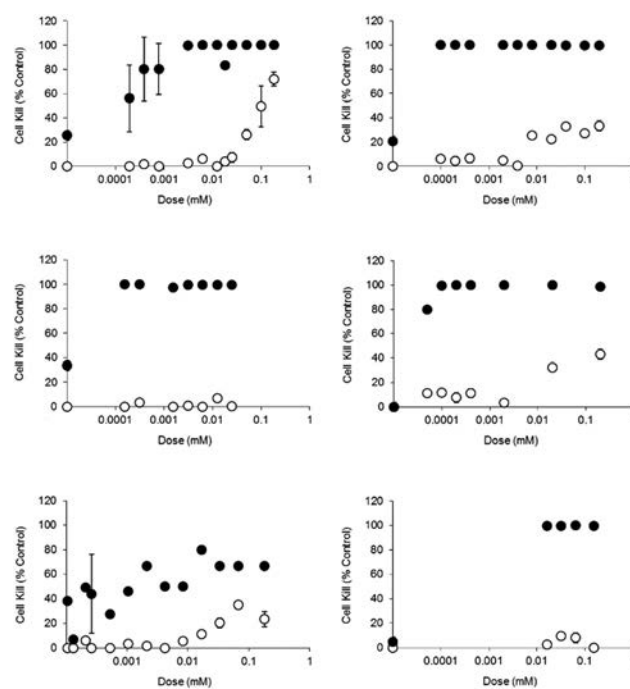


**Fig. 1** Dark (open circles) and light (filled circles) toxicity dose–response curves for TLD1411 (left column) and TLD1433 (right column) toward U87 (top), CT26.WT (middle) and F98 (bottom) cancer cell lines under *in vitro* normoxic conditions. Data are expressed as percentage kill versus control (no PS, no light). (Note: due to the sharp transition from no to complete cell kill, the standard deviation was large around the  $\text{LD}_{50}$ . For the remaining data points, the standard error is typically smaller than the symbol.)

**Table 1** LD<sub>50</sub> (μM) for TLD1411- and TLD1433-mediated PDT under normoxic conditions in 4 cancer cell lines *in vitro*. Note: 95% confidence intervals are presented in brackets for each LD<sub>50</sub>. Inverted therapeutic index (dark LD<sub>50</sub>/LD<sub>50</sub>) is also presented

	Cell lines				
	CT26.WT	CT26.CL25	U87	F98	
LD <sub>50</sub>	1411	0.57 (0.14–2.24)	NA	0.37 (0.17–0.80)	0.46 (0.17–1.24)
	1433	0.021 (0.005–0.087)	0.011 (0.002–0.073)	0.051 (0.019–0.14)	2.81 (0.18–41.94)
Inverted therapeutic ratio index (dark LD <sub>50</sub> /LD <sub>50</sub> )	1411	>44	NA	280	>397
	1433	>9709	>18 692	>3945	>54

1 μM for TLD1433. The resulting LD<sub>50</sub> for the two PSs and the 4 cell lines are listed in Table 1.

Under hypoxic conditions, Type I PSs are able to undergo photodynamic reactions by generating hydroxyl or other radicals either directly or indirectly, and thus retain their potential for killing cells in the absence of oxygen.<sup>1</sup> In contrast, Type II PSs can only undergo photodynamic reactions in the presence of oxygen and will, therefore, lose their efficacy under hypoxic conditions. The quantum yields for <sup>1</sup>O<sub>2</sub> production by TLD1411 and TLD1433 were close to unity, yet the PSs remained nonemissive in deoxygenated solutions (luminescence emission quantum yields of 0.0003 for TLD1411 and 0.0001 for TLD1433),<sup>29</sup> suggesting another nonradiative excited state quenching pathway that is very efficient in the absence of oxygen and might be exploited for PDT at low oxygen tension. To test the potential of these PSs to induce cell damage under hypoxic conditions, PDT with TLD1411 and TLD1433 was carried out *in vitro* on U87 cells under normoxic conditions (5% CO<sub>2</sub>, atmospheric O<sub>2</sub> and N<sub>2</sub> to balance) and under hypoxic conditions (0.5% O<sub>2</sub>, 5% CO<sub>2</sub>, N<sub>2</sub> to balance).

Under normoxic conditions, a strong photodynamic effect (above 70% cell kill) was observed for both TLD1411 and TLD1433 at 18 μM (Fig. 2). Dark toxicity was moderate for TLD1433 (~20% cell kill), whereas no dark toxicity was noted for TLD1411 (Fig. 1). Under hypoxic conditions, the PDT effect for both TLD1411 and TLD1433 was abolished, as was the PDT effect for aminolevulinic acid (ALA), an established oxygen-dependent PS. From these data, the LD<sub>50</sub> was estimated to be larger than 0.18 μM for the two PSs. The PDT effect mediated by the PSs was diminished in the presence of both hydroxyl radical and singlet oxygen scavengers (shown for TLD1433 in Fig. 3). Similarly, the PDT effect of ALA was eliminated in the presence of either of the scavengers.

*In vivo* MTD50 values were determined by applying a standard dose escalation scheme in the murine model, resulting in doses of 36 mg kg<sup>-1</sup> and 103 mg kg<sup>-1</sup> for TLD1411 and TLD1433, respectively. The administered doses for commonly used PSs are 12.5 mg kg<sup>-1</sup> for Photofrin and up to 200 mg kg<sup>-1</sup> for ALA in murine models,<sup>37</sup> so the clinically administered doses need to be lower for TLD1411 and TLD1433. It was observed that mice treated with doses above the MTD50 of TLD1411 demonstrated little to no immediate toxic effects within 24 hours but consistently showed signs of weakness, loss of appetite, ataxia, and death at 3–4 days post injection. Treatment with TLD1433 doses exceeding the MTD50 resulted

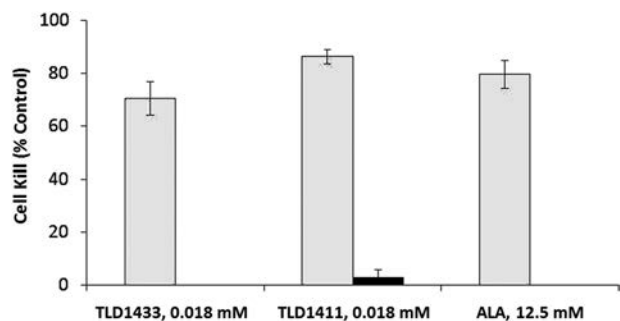


**Fig. 2** PDT effect of TLD1411 and TLD1433 in the U87 cancer cell line under normoxic (gray bars) and hypoxic (black bars) conditions (0.1–0.5% oxygen) compared to ALA, an established oxygen-dependent PS.

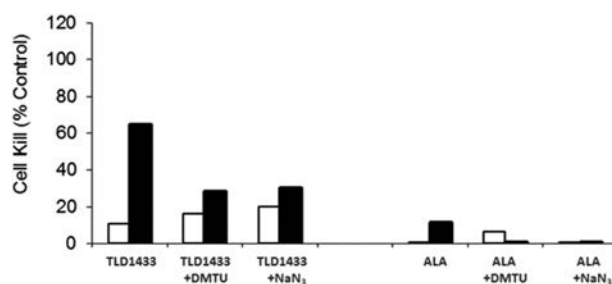


**Fig. 3** Cell kill by TLD1433 (20 μM) mediated PDT in the presence of the hydroxyl radical scavenger *N,N'*-dimethylthiourea (DMTU, 10 μM) or the singlet oxygen scavenger sodium azide (NaN<sub>3</sub>, 2 μM) in a U87 cancer cell line under *in vitro* normoxic conditions. 250 μM ALA was used as an oxygen-sensitive reference PS. Toxicity by the PS and the respective co-treatment without light (dark toxicity) are shown as white bars whereas true PDT effects after subtraction of the dark and light-only toxicities are presented as dark bars. Data are expressed as the number of cells killed as a percentage of the control (no PS, no light).

in neurological and behavioural symptoms (ataxia, abnormal gait) only within the first 24 hours post injection, and no death occurred when MTD50 was slightly exceeded.

At 4 hours post PS administration, liver and fecal matter showed the highest discolouration following IP administration during visual inspection at necropsy, whereas none of the skin samples showed detectable PS-associated discolouration. Four hours following intra-tumour injection, TLD1411 was detectable by tissue solubilisation and absorption based detection in

the spleen, but not in the other tissues. TLD1433 was not detectable in the heart, kidney, muscle, or spleen. At 24 hours both drugs were detectable only in tumour, liver and brain, suggesting rapid general clearance from the vasculature. Surprisingly, high levels of TLD 1411 were found in the brain at 4 hours ( $>100 \mu\text{M}$ ) and 24 hours ( $24.3 \mu\text{M}$ ), which was also true of TLD1433 ( $20.4 \mu\text{M}$  and  $11.5 \mu\text{M}$  at the same two time points). The concentrations in the liver were  $>100 \mu\text{M}$  for both photosensitizers and time points and, hence, outside of the assay's dynamic range. Tumour concentrations were lower for TLD1411 ( $3.73 \mu\text{M}$  and  $4.32 \mu\text{M}$  at 4 and 24 hours, respectively) in comparison to TLD1433 ( $30.8 \mu\text{M}$  and  $16.1 \mu\text{M}$  at 4 and 24 hours, respectively) whereby the difference cannot be explained solely by the difference in injected dose.

PDT has previously been shown to be effective in treating colon carcinomas in mouse models.<sup>38,39</sup> To determine the efficacy of PDT using TLD1411 and TLD1433 to cause growth delay in a C26WT subcutaneous tumour model, mice received IT injections with either TLD1411 or TLD1433 at two doses and were irradiated 4 hours post injection with either a cw or pulsed light source. Irradiation at  $190 \text{ J cm}^{-2}$  was delivered over 32 minutes in a 30 seconds on/off duty cycle to prevent heating of the hemoglobin in the capillaries (see Table 2 for all PDT parameters).

The tumours in PDT treated mice were significantly reduced or undetectable 24 hours post treatment for the treatment conditions in Table 1. For TLD1411 at  $2 \text{ mg kg}^{-1}$ , an average tumour growth delay of 8 days ( $p = 0.15$ ) was observed; however, all tumours recurred. PDT with  $5 \text{ mg kg}^{-1}$  of TLD1433 resulted in an average growth delay of 9 days ( $p < 0.05$ ), with a statistically significant survival advantage.

Fig. 4 and 5 present the animal survival following cw and pulsed light sources with TLD1411 and TLD1433 at the low and high photosensitizer doses according to Table 2, respectively. The analysis of the Kaplan–Meier survival curves shows that there was a significant increase in animal survival with  $36 \text{ versus } 2 \text{ mg kg}^{-1}$  TLD1411 doses using a cw light source *versus* light-only and PS-only control mice ( $p < 0.01$ ). Similarly, TLD1433 showed a significant increase in animal survival with the higher TLC doses using the cw light source ( $p < 0.05$ ).

**Table 2** PDT parameters for *in vivo* experiments

PS	PS dose	Light dose	# Mice
TLD1411	$36 \text{ mg kg}^{-1}$	cw, $192 \text{ J cm}^{-2}$ , $200 \text{ mW cm}^{-2}$	4
	$36 \text{ mg kg}^{-1}$	Pulse, $192 \text{ J cm}^{-2}$ , $200 \text{ mW cm}^{-2}$	6
	$2 \text{ mg kg}^{-1}$	cw, $192 \text{ J cm}^{-2}$ , $200 \text{ mW cm}^{-2}$	5
	$2 \text{ mg kg}^{-1}$	Pulse, $192 \text{ J cm}^{-2}$ , $200 \text{ mW cm}^{-2}$	5
TLD1433	$53 \text{ mg kg}^{-1}$	cw, $192 \text{ J cm}^{-2}$ , $200 \text{ mW cm}^{-2}$	3
	$53 \text{ mg kg}^{-1}$	Pulse, $192 \text{ J cm}^{-2}$ , $200 \text{ mW cm}^{-2}$	6
	$5 \text{ mg kg}^{-1}$	cw, $192 \text{ J cm}^{-2}$ , $200 \text{ mW cm}^{-2}$	7
	$5 \text{ mg kg}^{-1}$	Pulse, $192 \text{ J cm}^{-2}$ , $200 \text{ mW cm}^{-2}$	5

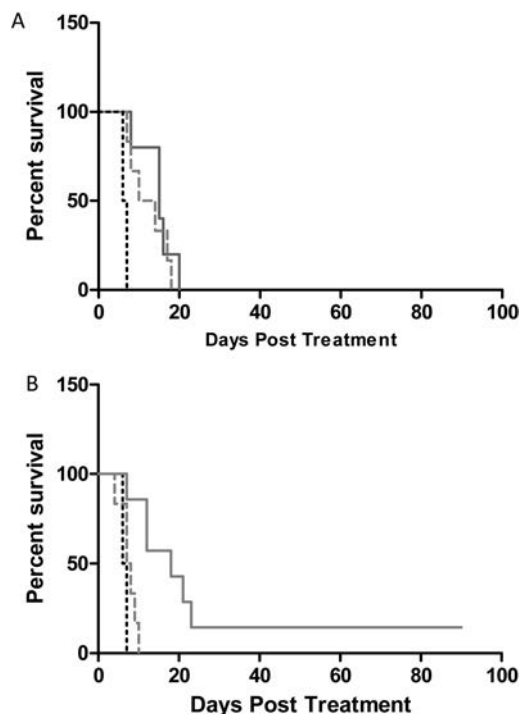


**Fig. 4** Kaplan–Meier survival curves of mice bearing tumours post TLD1411- or TLD1433-mediated PDT using a cw light source: (A) TLD1411 ( $1/10 \text{ MTD}_{50} - 2 \text{ mg kg}^{-1}$ ). Light only (black dotted), TLD1411 only (grey dashed), TLD1411 plus cw: light (grey solid). (B) TLD1433 ( $1/20 \text{ MTD}_{50} - 5 \text{ mg kg}^{-1}$ ). Light only (black dotted), TLD1433 only (grey dashed) and TLD1433 plus cw light (grey solid).

## Discussion

Our study explored the effectiveness of two PSs in the destruction of cancer cells both *in vitro* and *in vivo*. TLD1411 and TLD1433 are mononuclear, Ru(II)-based, low molecular weight ( $<2 \text{ kDa}$ ) synthetic coordination complexes that have a high inherent resistance to photobleaching and exhibit remarkable  $^1\text{O}_2$  quantum yields (approximately 1, so that the luminescence quantum yield is  $<0.001$ ). These properties make TLD1411 and TLD1433 favourable Type II PS candidates. It is noteworthy that *in vitro* PDT-mediated cell death was demonstrated in a range of concentrations that were at least two magnitudes lower than the concentrations where notable dark toxicity was observed. The  $\text{LD}_{50}$  of TLD1433 was significantly ( $p < 0.05$ ) lower than that of TLD1411 for CT26.WT and U87 cell lines, demonstrating a much higher PDT efficacy of TLD1433. The differences in  $\text{LD}_{50}$  for either TLD1411 or TLD1433 between the three wavelengths are due to different accumulation of the photosensitizers between these cell lines and also the inherent sensitivity of these cell lines to the cytotoxins generated during PDT, not unlike other photosensitizers.<sup>40</sup>

A comparison with the *in vitro* PDT activity of other Ru(II) complexes previously presented in the literature is not possible due to the use of either white light illumination, activating typically multiple transitions in these complexes, the large variability in the drug-light interval affecting biodistribution,

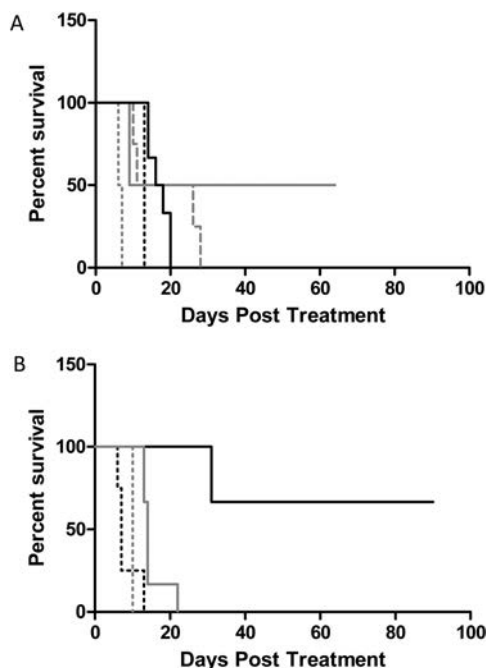


**Fig. 5** Kaplan–Meier survival curves showing the effects of PDT with TLD1411 or TLD1433 at 1/2 MTD50 doses for TLD1411 and TLD1433 using cw (525 nm) versus pulsed (532 nm) light sources: (A) cw light only (black dotted), pulse light only (grey dotted), TLD1411 (19 mg kg<sup>-1</sup>) only (grey dashed), light source: cw (black solid) and pulsed (grey solid); (B) cw light only (black dotted), pulse light only (grey dotted), TLD1433 (53 mg kg<sup>-1</sup>), light source: cw (black solid) and pulsed (grey solid).

and the cell lines used. However, the demonstrated dark toxicity up to the mM range and light toxicity down to the nM range are comparable to the available reports. This impressive *in vitro* therapeutic ratio needs to be taken with caution due to the high photostability of these complexes (see ESI Fig. 3†), as a reduced drug concentration can be exchanged with an increased radiant exposure.

In planktonic cultures it was shown that TLD1433 possesses the ability to act as both a photo-oxidant and a photo-reductant *via* their excitation stage, enabling Type I photoprocesses in hypoxic environments or in the presence of efficient <sup>1</sup>O<sub>2</sub> scavengers.<sup>23</sup> They incorporate the IP-TT ligand that imparts a non-linear optical capacity for two-photon absorption, which can be controlled further by the identity of the ancillary ligands. Thus, the Ru-based PSs have the potential to act as a Type I or Type II PS toward DNA isolates in response to oxygen tension<sup>30</sup> also confirmed by their efficacy in bacteria cell kill.<sup>29</sup> However, it is not guaranteed that this DNA based activity in eukaryotic cell culture will be present also in mammalian cell cultures *in vitro* or *in vivo*. While previous studies by us<sup>29</sup> and others<sup>21,28,30</sup> have emphasized the high affinity of these two and other Ru(II) complexes for DNA, it is important to note that these experiments were completed using DNA plasmid in solution. Initial *in vitro* imaging studies<sup>28</sup> showing some potential nuclear accumulation do not seem to hold for all the treatment conditions and cell lines, and ongoing studies also show a probable cytoplasmic accumulation (data not shown

and work in progress). However, should nuclear localization be observed under particular treatment conditions considered for clinical translation, detailed studies pertaining to the mutagenic effects of surviving normal and cancer cells are required. Indeed, both TLD1411 and TLD1433 were rendered ineffective under hypoxic conditions, and the presence of hydroxyl radical and singlet oxygen scavengers strongly diminished the effectiveness of PDT mediated by TLD1411 and TLD1433. These results suggest a predominant Type II photoprocess for both of the evaluated PSs. Cell kill based on the generation of DNA intercalating species or direct DNA single and double strand generation was not evaluated in this study.

The biodistribution study shows very rapid clearing of the photosensitizers from most tissues in less than 24 hours with the exception of liver, tumour and the brain (data not shown). The latter could potentially be due to the retention of the PSs by the blood–brain barrier. Liver retention is not surprising as it appears to be the principal path for elimination of the drug.<sup>41</sup> The tumour retention is modest for IP and also IT injections, indicating that for direct injection shorter incubation time points should be considered.

In the presence of targets for the PDT generated ROS, TLD1411 and TLD1433 showed remarkable stability. In fact, the initial loss of 30% absorbance during the early points of the total radiant exposure did not modify the overall PDT response.

Light of 532 nm creates a very strong fluence rate gradient inside tissue as haemoglobins and cytochromes are strong absorbers with molar extinction coefficients of 33 644 M<sup>-1</sup> cm<sup>-1</sup> (haemoglobin, Hb), 45 680 M<sup>-1</sup> cm<sup>-1</sup> (oxyhaemoglobin, HbO)<sup>42</sup> and 8210.8 M<sup>-1</sup> cm<sup>-1</sup> (cytochrome C).<sup>28</sup> Therefore, effective attenuation coefficients are reported for weakly (skin, ~6.9–8.1 cm<sup>-1</sup>) and strongly (~20 cm<sup>-1</sup>, tumour) perfused tissues. Assuming a skin thickness of 0.7 mm and a tumour of 3 mm depth, 2–10 J cm<sup>-2</sup> would reach the tumour base when delivering 192 J cm<sup>-2</sup> radiant exposure as in this model.

The effect of PDT was found to be highly dependent on the doses of TLD1411 and TLD1433 and/or the activating light sources. For equal radiant exposure at 525 nm cw and 532 nm pulsed there was a significant difference in *in vivo* treatment response. The irradiation with light alone and the IT administration of TLD1411 and TLD1433 alone had no effect on tumour growth.

Kaplan–Meier plots showed a significant increase in animal survival with TLD1411 in 19 mg kg<sup>-1</sup> and 2 mg kg<sup>-1</sup> doses using a cw light source in comparison to light-only or PS-only control mice (*p* < 0.01). TLD1433 PDT showed significant tumour damage and delay in tumour growth in a dose-dependent manner. Similarly, TLD1433 showed a significant increase in animal survival with 53 mg kg<sup>-1</sup> and 5 mg kg<sup>-1</sup> dose using the cw light source (*p* < 0.05).

As the PSs are not subject to photobleaching, the tissue response can be further augmented by increasing the radiant exposure. This needs to be considered for the clinical translation, particularly if the tumour selectivity is maintained.

## Conclusion

These studies demonstrate that Ru(II) PSs are suitable for oncological applications despite their short activation wavelength. Their high level of photostability permits the delivery of a very high radiant exposure which assists in overcoming the strong fluence rate gradient in tissues. Additionally these Ru(II) PSs exhibit very high single oxygen quantum yields for well oxygenated tissue; thus the delivery of an effective PDT dose can be achieved by adjusting the photon density to the available oxygen in the target tissue.

## Acknowledgements

This study was supported in part by the Ontario Ministry of Health and Long Term Care and by Theralase Inc. The authors would like to express their thanks to S. Monro, G. Shi, and Dr S. McFarland for the preparation and synthesis of the photosensitizers as well as Drs R. Hill and B. Wouters for the use of their hypoxic chamber.

## References

- 1 P. Agostinis, *et al.*, Photodynamic therapy of cancer: an update, *CA: Cancer J. Clin.*, 2011, **61**, 250–281.
- 2 A. P. Castano, P. Mroz and M. R. Hamblin, Photodynamic therapy and anti-tumour immunity, *Nat. Rev. Cancer*, 2006, **6**, 535–545.
- 3 D. E. J. G. J. Dolmans, D. Fukumura and R. K. Jain, Photodynamic therapy for cancer, *Nat. Rev. Cancer*, 2003, **3**, 380–387.
- 4 L. Lilje, M. Portnoy and B. C. Wilson, Apoptosis induced in vivo by photodynamic therapy in normal brain and intracranial tumour tissue, *Br. J. Cancer*, 2000, **83**, 1110–1117.
- 5 P. Mroz, *et al.*, Imidazole metalloporphyrins as photosensitizers for photodynamic therapy: role of molecular charge, central metal and hydroxyl radical production, *Cancer Lett.*, 2009, **282**, 63–76.
- 6 A. E. O'Connor, W. M. Gallagher and A. T. Byrne, Porphyrin and nonporphyrin photosensitizers in oncology: preclinical and clinical advances in photodynamic therapy, *Photochem. Photobiol.*, 2009, **85**, 1053–1074.
- 7 M. Ethirajan, Y. Chen, P. Joshi and R. K. Pandey, The role of porphyrin chemistry in tumor imaging and photodynamic therapy, *Chem. Soc. Rev.*, 2011, **40**, 340–362.
- 8 A. Casini, C. G. Hartinger, A. A. Nazarov and P. J. Dyson, in *Medicinal Organometallic Chemistry*, ed. G. Jaouen and N. Metzler-Nolte, Springer, Berlin, Heidelberg, 2010, vol. 32, pp. 57–80.
- 9 C. L. Evans, *et al.*, Killing hypoxic cell populations in a 3D tumor model with EtNBS-PDT, *PLoS One*, 2011, **6**, e23434.
- 10 T. Gallavardin, *et al.*, Photodynamic therapy and two-photon bio-imaging applications of hydrophobic chromophores through amphiphilic polymer delivery, *Photochem. Photobiol. Sci.*, 2011, **10**, 1216–1225.
- 11 S. Anand, B. J. Ortel, S. P. Pereira, T. Hasan and E. V. Maytin, Biomodulatory approaches to photodynamic therapy for solid tumors, *Cancer Lett.*, 2012, **326**, 8–16.
- 12 J. T. Hashmi, *et al.*, Effect of pulsing in low-level light therapy, *Lasers Surg. Med.*, 2010, **42**, 450–466.
- 13 N. Vardeny, *et al.*, Photogeneration of confined soliton pairs (bipolarons) in polythiophene, *Phys. Rev. Lett.*, 1986, **56**, 671–674.
- 14 W. T. Eckenhoff, W. W. Brennessel and R. Eisenberg, Light-Driven Hydrogen Production from Aqueous Protons using Molybdenum Catalysts, *Inorg. Chem.*, 2014, **53**, 9860–9869.
- 15 L. Zhang, Y. Gao, X. Ding, Z. Yu and L. Sun, High-Performance Photoelectrochemical Cells Based on a Binuclear Ruthenium Catalyst for Visible-Light-Driven Water Oxidation, *ChemSusChem*, 2014, **7**, 2801–2804.
- 16 C. Mari, *et al.*, DNA Intercalating Ru II Polypyridyl Complexes as Effective Photosensitizers in Photodynamic Therapy, *Chem. – Eur. J.*, 2014, **20**, 14421–14436.
- 17 E. Wachter, D. K. Heidary, B. S. Howerton, S. Parkin and E. C. Glazer, Light-activated ruthenium complexes photobind DNA and are cytotoxic in the photodynamic therapy window, *Chem. Commun.*, 2012, **48**, 9649–9651.
- 18 B. S. Howerton, D. K. Heidary and E. C. Glazer, Strained ruthenium complexes are potent light-activated anticancer agents, *J. Am. Chem. Soc.*, 2012, **134**, 8324–8327.
- 19 A. A. Holder, D. F. Ziegler, M. T. Tarrago-Trani, B. Storrie and K. J. Brewer, Photobiological impact of [(bpy)2Ru(dpp)]2RhCl2]Cl5 and [(bpy)2Os(dpp)]2RhCl2]Cl5 [bpy=2,2'-bipyridine; dpp=2,3-Bis(2-pyridyl)pyrazine] on vero cells, *Inorg. Chem.*, 2007, **46**, 4760–4762.
- 20 R. B. Sears, *et al.* Photoinduced ligand exchange and DNA binding of cis-[Ru(phpy)(phen)(CH3CN)2]+ with long wavelength visible light, *J. Inorg. Biochem.*, 2013, **121**, 77–87.
- 21 Y. Chen, *et al.*, Fusion of photodynamic therapy and photo-activated chemotherapy: a novel Ru(II) arene complex with dual activities of photobinding and photocleavage toward DNA, *Dalton Trans.*, 2014, **43**, 15375–15384.
- 22 H. Yin, *et al.*, In vitro multiwavelength PDT with 3IL states: teaching old molecules new tricks, *Inorg. Chem.*, 2014, **53**, 4548–4559.
- 23 Y. Liu, *et al.*, Ru(II) complexes of new tridentate ligands: unexpected high yield of sensitized 1O2, *Inorg. Chem.*, 2009, **48**, 375–385.
- 24 Q.-X. Zhou, *et al.*, [Ru(bpy)(3-n)(dpp)(n)](2+): unusual photophysical property and efficient DNA photocleavage activity, *Inorg. Chem.*, 2010, **49**, 4729–4731.
- 25 A. Levina, A. Mitra and P. A. Lay, Recent developments in ruthenium anticancer drugs, *Met. Integr. Biometal Sci.*, 2009, **1**, 458–470.
- 26 Z. Huang, *et al.*, Photodynamic therapy for treatment of solid tumors—potential and technical challenges, *Technol. Cancer Res. Treat.*, 2008, **7**, 309–320.
- 27 R. Lincoln, *et al.*, Exploitation of long-lived 3IL excited states for metal-organic photodynamic therapy: verification

- tion in a metastatic melanoma model, *J. Am. Chem. Soc.*, 2013, **135**, 17161–17175.
- 28 G. Shi, *et al.*, Ru(II) dyads derived from  $\alpha$ -oligothiophenes: A new class of potent and versatile photosensitizers for PDT, *Coord. Chem. Rev.*, 2015, **282**, 127–138.
- 29 Y. Arenas, *et al.*, Photodynamic inactivation of *Staphylococcus aureus* and methicillin-resistant *Staphylococcus aureus* with Ru(II)-based type I/type II photosensitizers, *Photodiagn. Photodyn. Ther.*, 2013, **10**, 615–625.
- 30 S. Monro, *et al.*, Photobiological activity of Ru(II) dyads based on (pyren-1-yl)ethynyl derivatives of 1,10-phenanthroline, *Inorg. Chem.*, 2010, **49**, 2889–2900.
- 31 W. E. Jones, R. A. Smith, M. T. Abramo, M. D. Williams and J. Van Houten, Photochemistry of hetero-tris-chelated ruthenium(II) polypyridine complexes in dichloromethane, *Inorg. Chem.*, 1989, **28**, 2281–2285.
- 32 L. Lilge, C. O'Carroll and B. C. Wilson, A solubilization technique for photosensitizer quantification in ex vivo tissue samples, *J. Photochem. Photobiol., B*, 1997, **39**, 229–235.
- 33 T. S. Istivan, *et al.*, Biological effects of a de novo designed myxoma virus peptide analogue: evaluation of cytotoxicity on tumor cells, *PLoS One*, 2011, **6**, e24809.
- 34 J. M. Suflita and F. Concannon, Screening tests for assessing the anaerobic biodegradation of pollutant chemicals in subsurface environments, *J. Microbiol. Methods*, 1995, **21**, 267–281.
- 35 V. Baumans, P. F. Brain, H. Burgere, P. Clausing, T. Jeneskog and G. Perretta, Pain and distress in laboratory rodents and lagomorphs. Report of the Federation of European Laboratory Animal Science Associations (FELASA) Working Group on Pain and Distress accepted by the FELASA Board of Management November 1992, *Lab. Anim.*, 1994, **28**, 97–112.
- 36 S. Robinson, *et al.*, *Guidance on dose level selection for regulatory general toxicology studies for pharmaceuticals*, at <http://www.lasa.co.uk/PDF/LASA-NC3RsDoseLevelSelection.pdf>.
- 37 Q. Peng, *et al.*, Antitumor effect of 5-aminolevulinic acid-mediated photodynamic therapy can be enhanced by the use of a low dose of photofrin in human tumor xenografts, *Cancer Res.*, 2001, **61**, 5824–5832.
- 38 P. Mroz, A. Szokalska, M. X. Wu and M. R. Hamblin, Photodynamic therapy of tumors can lead to development of systemic antigen-specific immune response, *PLoS One*, 2010, **5**, e15194.
- 39 R. Sanovic, T. Verwanger, A. Hartl and B. Krammer, Low dose hypericin-PDT induces complete tumor regression in BALB/c mice bearing CT26 colon carcinoma, *Photodiagn. Photodyn. Ther.*, 2011, **8**, 291–296.
- 40 C. J. Fisher, *et al.*, Modulation of PPIX synthesis and accumulation in various normal and glioma cell lines by modification of the cellular signaling and temperature: modulation of PPIX synthesis, *Lasers Surg. Med.*, 2013, **45**, 460–468.
- 41 C. Scolaro, *et al.*, In vitro and in vivo evaluation of ruthenium(II)-arene PTA complexes, *J. Med. Chem.*, 2005, **48**, 4161–4171.
- 42 U. Heinrich, *Untersuchungen zur qualitativen photometrischen analyse der redox-zustande der atmungskette in vitro und in vivo am beispiel des gehirns*, Abteilung fur Biologie and der Ruhr-Universitat Bochum, 1981.